ORIGINAL PAPER

Eco-friendly neem leaf-based activated carbon for methylene blue removal from aqueous solution: adsorption kinetics, isotherms, thermodynamics and mechanism studies

Uttam Kumar Sahu[1] · Swagatika Tripathy[2] · Narayan Gouda[3] · Hari Sankar Mohanty[4] · Bodala Dhannjaya[1] · Vinod Kumar Choudhury[1] · Abinash Sahu[1] · Anil Gouda[1]

Abstract

Using biomass materials for activated carbon preparation through a simple and expedient method is a highly appropriate approach for sustainable and green development. Here, for the first time the waste neem (*Azadirachta Indica*) leaf was used for the development of activated carbon in the microwave process assisted with K_2CO_3 as an activating agent, and its performance was checked for methylene blue dye (MB) removal. The neem leaves activated carbon (NLAC) was analyzed with sophisticated instrument, where the SEM, XRD and pH_{IEP} results showed that NLAC surface has highly active pores, is crystalline in nature and has a pH_{IEP} value of 6.9. The FTIR data indicated that a number of active functional groups (–OH, –COOH, etc.) were present on the NLAC surface. The BET data presented that material has a good surface area of 50.69 m^2/g and a pore volume of 0.014 cm^3/g. More than 96% of MB dye was removed in the obtained environments of 10 mg/L MB dye concentration, pH 7, contact time 100 min, adsorbent dose of 70 mg and temperature 80 °C, respectively. The removal data were suitably followed by Langmuir isotherm model ($R^2 = 0.96$) having an uptake capacity of 132.52 mg/g. Kinetics data for MB removal were matched with the pseudo-second-order model with a R^2 of 0.96. The adsorption process was spontaneous in nature, where ΔH and ΔS values were 0.029 kJ/mol and 0.095 kJ/Kmol. The adsorption mechanism was followed by three types of interaction, i.e., electrostatic attraction, hydrogen bonding and pi–pi interaction, respectively.

Keywords Neem leaf · Activated carbon · Methylene blue · Adsorption and removal

Introduction

Environmental balance is the key for the existence of human and aquatic life. But due to a rapid increase in global population and industrialization, the balance of ecosystem ruptures and in near future creates a lot of problems for the living organism [1]. Recent studies signify that the degradation of surface water quality creates an imbalance in the ecosystem and indirectly brings the global warming [2], agricultural shortfall [3] and health complications [4]. This surface water loses its purity mainly because of untreated disposal of wastes from the industries which are full of toxic materials including heavy metals, pharmaceutical products and color organic dyes. Mainly, the dyes in the water are the major pollutants with greater poisoning trails and every year 200,000 tons organic dyes are disposed into the surface water and make it unusable [5, 6]. Among different types of dyes, methylene blue (cationic dye) is broadly utilized in the textile, paper and carpet industries and also has extensive application in the food, pharmaceutical, fabric, leather and cosmetics production [7]. This MB dye normally has complicated aromatic molecular systems which made them to be extra stable and extra hard to biodegrade in the natural environment [8]. The removal of this color is highly essential as it generates problems in esthetic deterioration

✉ Uttam Kumar Sahu
  sahuuttam02@gmail.com

[1] Department of Chemistry, GIET University, Gunupur, Odisha 765022, India

[2] Department of Chemistry, Veer Surendra Sai University of Technology, Burla, Odisha 768018, India

[3] School of Applied Sciences, Department of Chemistry, Centurion University of Technology and Management, Parlakhemundi, Odisha 761211, India

[4] Department of Physics, GIET University, Gunupur, Odisha 765022, India

penetration of dissolved oxygen and daylight into water bodies, which severely influences the aquatic life. Besides this, the dye precursors and degradation products are verified as carcinogenic and mutagenic [9]. Consumption of MB dye-polluted water can be the reason for hypersensitive reactions, dermatitis, pores and skin irritation, and most cancers with mutations in infants and matures [10].

Many powerful strategies have been used to get clean water from wastewater, which include ozonation [11], chemical coagulation [12], precipitation [13], oxidation [14], reverse osmosis [15], photoabsorber [16, 17], photocatalytic water oxidation [18, 19] and degradation [20]. Some of these techniques have a large number of chemical uses, sensitivity to a variable wastewater input, steeply priced plant necessities with operational costs and accumulation of focused sludge with disposal problems. One of the effective and convenient toxic pollutants' remediation methods is adsorption, which shows high accuracy with good output results without any secondary pollutants formation [21]. Hence, a lot of researchers have used adsorption techniques for toxic dye [22], heavy metal [22] and organic pollutants [23] removal. Choosing of adsorbent in the adsorption process also played an important role as it is directly associated with economic factors and practical application. Therefore, researchers have chosen activated carbon for MB dye removal from wastewater. The properties like high surface area, reusability, higher mesoporous binding sites and good stability under acidic and basic environments make it unique than other adsorbents [24]. However, the commercial activated carbon which is available in the market has a very high cost and limits its application on large scales [25]. To solve these problems, several studies have been conducted where plant-based materials like lychee seed [26], gulmohar fruit shell [27] and orange peel [28] are used for activated carbon preparation and applied for MB dye removal. Here, the activating agents KOH and H_3PO_4 have been used for lychee seed and gulmohar fruit activated carbon preparation and found good results. However, these reagents are not highly soluble and stable in water environments. Lastly, the orange peel is simply used without any modification, which limits its application toward the removal of MB dye. Khairunnadhrah Jasri et al. have used oil palm frond and palm kernel shell for activated carbon preparation and found that 96% of MB dye has been removed, and the materials have an uptake capacity of 331.6 mg/g [29]. Irwan Kurnia and co-worker have used coconut shell for activation carbon preparation in thermal process (350 °C) and applied for MB removal. They found that the material has an adsorption capacity of 160.36 mg/g in the optimized condition [30]. Dodonaea viscosa fruit has been used for activated carbon preparation by Asim Yaqub et al. with MB dye uptake capacity of 370 mg/g. In another research, walnut shell has been used for activated carbon preparation by the thermal process (700–1000 °C). This activated carbon is highly efficient with a surface area of 903.9 m^2/g and a good uptake capacity of 307.4 mg/g, respectively

[31]. Hence, these studies indicate that the low cost, easily available, environmental friendly agricultural products can be potentially applied as a source for activated carbon preparation and effectively applied for MB dye removal from water with high adsorption capacities.

Generally, two methods are used for activated carbon preparation: physical method and chemical method. It is found that the chemical method using the activating agent like $ZnCl_2$, KOH, H_3PO_4, K_2CO_3, NaOH and HNO_3 under an inert atmosphere is more convenient for activated carbon preparation [32]. But studies show that using K_2CO_3 as an agent, the prepared activated carbon has a high surface area with higher oxygen carrier functional groups, and an environmentally friendly nature [33]. Therefore, a lot of studies have been done where K_2CO_3 is used as an agent for activated carbon preparation and used for dye decolorization [34], pesticide removal [35] and CO_2 adsorption [36], respectively.

Neem (*Azadirachta indica*) of the Meliaceae family is a commonly available plant in Asian countries [37, 38]. The fruits, leaves, roots and branches of neem tree are frequently applied for therapeutic cures like digestive disorders control, maintain diabetes and cholesterol levels. Neem is also used in the field of cosmetics, fertilizer, pesticides, lubrication, etc. [39]. Hence, neem plant materials are used in many ways and after being used their waste materials are thrown to the dustbin.

In this work, for the first time the waste neem leaf was used for activated carbon preparation and used for MB dye removal from aqueous solution. The use of K_2CO_3 as an activating agent has improved the surface structure of activated carbon as it has properties like readily soluble in water and forming resilient alkaline solution, low price and easily available everywhere. The activated carbon synthesized in the microwave technique is an utmost desirable process because of its less energy consumption in a shorter time and homogeneous distribution of heat [40]. The feasibility of the prepared NLAC was checked for the adsorption of MB dye using a batch removal study. The influential parameters such as pH, adsorbent dose, initial concentration, temperature and contact duration were analyzed in batch studies. The adsorption chemical kinetics and isotherm analyses were directed, and lastly, the MB dye adsorption mechanism on NLAC has been proposed in this study.

Experimentations

Materials

All chemicals were of analytical grade and directly used without any further purification. Methylene blue ($C_{16}H_{18}ClN_3S$) dye and potassium carbonate (K_2CO_3) were

taken from Merck and HiMedia Chemicals (India). The waste neem leaves (NL) were taken from the neem trees of the GIET University campus. The NL was washed 3 times with deionized water to take away dust. The impurities are soluble in water, and they were dried until the neem leaves become crisp. The dried neem leaves had been crushed and powered and then washed with deionized water until the washing had been freed from turbidity and color. Then, the NL powder is stirred with 0.1 M sulfuric acid for 30 min, and then again it was washed three times with deionized water to remove untreated acid and dried at 100 °C and positioned in a desiccator. Thereafter, the dried NL were crushed into fine powder of size 1–2 mm.

Preparation of adsorbent

The dried NL were first carbonized in a tube furnace for 2 h in a nitrogen atmosphere at the temperature of 800 °C and the selected ramp of temperature was 5 °C/min. After succeeding carbonization, the product was dissolved in K_2CO_3 solutions (impregnation ratio 1:2). Then, this product solution was moved to microwave activation under a nitrogen atmosphere at 800 W for 10 min. On completion of activation, the solution was washed with deionized water until it reached neutral, and the washed sample was dried at 100 °C with the help of a hot air oven for one day and that sample was mentioned as neem leaves activated carbon (NLAC).

Instrumental analysis

Phase and crystallographic states of NL and NLAC were detected using an X-ray diffractometer (RIGAKU JAPAN/ ULTIMA-IV) having Cu-kα radiation. The functional groups present on NL and NLAC before and after MB adsorption were analyzed with the FTIR spectrometer (RXI, PerkinElmer, USA). Raman bands were identified with the help of the Ranishawin Viarelex spectrometer. MALVERN ZS 90 zeta potential instrument was used to calculate the surface charge of NLAC at different pH. The surface morphology of NL and NLAC before and after adsorption was pasteurized using a scanning electron microscope (JSM-6390LV, JEOL Model, Japan). The surface area with other surface properties (pore volume and pore size) of NL and NLAC was calculated with a Quantachrome surface area analyzer. Lastly, the MB concentration after adsorption was examined with the UV–visible spectrophotometer (UV-2540).

Batch adsorption studies

For batch adsorption, the initial stock solution was prepared by dissolving 0.0373 g of MB dye in 100 ml deionized water. An experimental solution of the favored concentration has been received through dilutions of this stock solution

in distilled water. The batch adsorption studies were conducted in 50 mL dye solution with different concentrations (10–100 mg/L). The required adsorbent dose was added to the dye solution and shaken for 180 min at 300 rpm. pH of the solution was maintained with 0.1 M NaOH and HCl solution. After adsorption, the adsorbent was separated by the centrifugation method and the residual dye concentration and uptake capacity are calculated with the help of the following equation:

$$R(\%) = \frac{\text{Co} - \text{Ce}}{\text{Co}} \times 100 \qquad (1)$$

$$q_e = \frac{\text{Co} - \text{Ce}}{W} \times V \qquad (2)$$

where Co and Ce are the initial and equilibrium concentrations (both in mg/L); q_e (mg/g) represents the adsorbent uptake capacity; V (L) and W (g) are the volume of solution and adsorbent weight; and R (%) indicates the percentage of removal, respectively.

Results and discussion

Characterizations of adsorbent

XRD

By X-ray diffraction, the crystallography depiction of activated carbon prepared from neem leaf waste has been analyzed. The XRD peaks of NL and NLAC before and after MB adsorption are presented in Fig. 1. Both NL and NLAC showed several peaks detected at 24.97°, 29.50°, 36.13°, 39.72°, 43.50° and 48.25° for 400, 238, 418, 274, 574 and 214 planes, respectively. This indicated that NLAC prepared from NL was crystalline. The presence of peaks at 24.97 and 43.50 (represented by circle) corresponded to activated carbon as reported by other researchers [41]. The presence of other peaks in NLAC was mainly due to the presence of mineral content (Mg, Na, Fe, Ca, Cu and Zn) on the activated carbon surface [38]. After MB adsorption, the NLAC peaks became smoother with a change in intensities. Overall, it was found that the merger of MB on the NLAC surface did not change the crystal phases.

FTIR

The results obtained from FTIR studies of NL and NLAC before and after MB adsorption are presented in Fig. 2. NL has a broad bend at 3308 cm^{-1} which was mainly for –OH stretching vibrational mode of phenol, acid and alcohol, respectively. Again, a bend at 1579 cm^{-1} was seen for
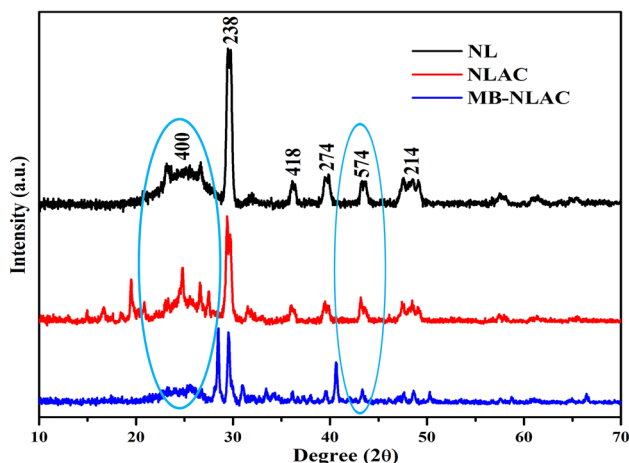
Fig. 1 XRD patterns of NL, NLAC and MB dye-adsorbed NLAC

stretching vibration of C=C present in the aromatic benzene compound [26]. But after modification and activated carbon formation, the –OH vibrational band at 3308 cm^{-1} was shifted to 3358 cm^{-1} and became much smoother. The pick at 1580 cm^{-1} was noticed, and the bend raised at 1178 cm^{-1} was for C–O bending vibrations of phenol, ether and alcohol groups [27]. The FTIR spectrum of NLAC was entirely transformed and some new peaks appeared after the adsorption of MB dye. Several new bends were found in between 1365 and 741 cm^{-1} (represented by circle) which resembled N=O, C–N and C=O groups. The broad band at 3358 cm^{-1} was shifted to 3416 cm^{-1}, and the bend at 1580 cm^{-1} was completely removed. Hence, the shifting, omitting and arise
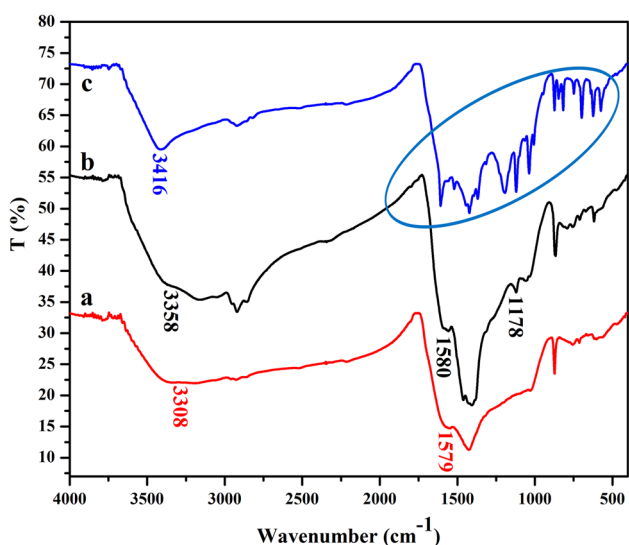
of new peaks confirmed that MB dyes were attached to the NLAC surface and removed from the solution.

Raman

Figure 3 shows the Raman spectrum of NL and NLAC before and after MB adsorption. In all the cases, two broad bands at 1358 and 1587 cm^{-1} were depicted as D and G bends, respectively. The ratios of D to G bend for NL and NLAC before and after MB adsorption were 0.87, 0.91 and 0.93, respectively. This indicated that disorderliness in the material increased after activated carbon formation and MB dye adsorption. Hence, the activated carbon prepared from NL was provided with higher active binding sites and therefore interaction occurred with the MB dyes and was effectively eliminated from the solution.

Zeta potential analysis

The surface charge of the adsorbent plays a key role in the adsorption process, so the zeta potential study has been done for NLAC and is presented in Fig. 4. The pH$_{IEP}$ of activated carbon was 6.9; hence, the adsorbent surface became negatively charged above this pH and suitable for interaction with positively charged MB dye present in the aqueous solution.

SEM and EDX

SEM micrographs of the NL and NLAC before and after MB adsorption are presented in Fig. 5. The NL didn't have any uniform fixed morphology where both small pores and smooth surfaces were present. But the NLAC had a high number of pores and the surface looked like a symmetrical
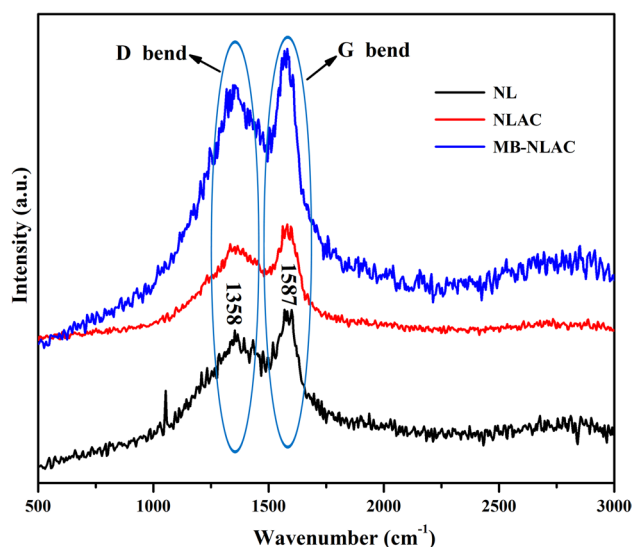

Fig. 2 FTIR spectra of NL (**a**) and NLAC before (**b**) and after (**c**) MB dye adsorption

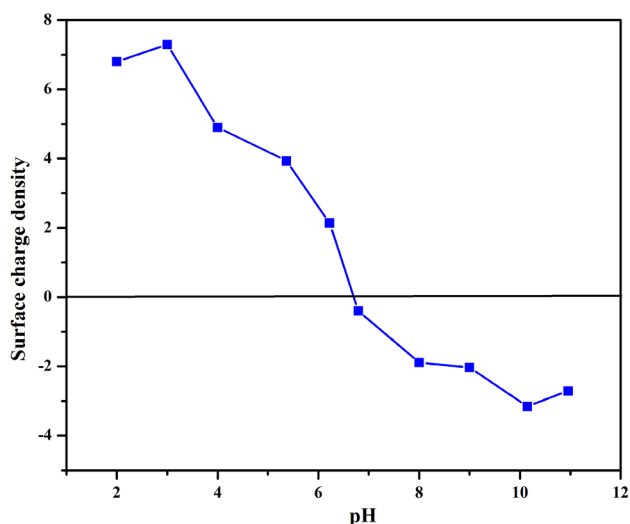**Fig. 3** Raman spectrum of NL, NLAC and MB dye-adsorbed NLAC

Fig. 4 Surface charge density of NLAC at different pH

macro-meso pore and some large holes (cavities) which may be allowed for the diffusion of the MB dye molecule. The K_2CO_3 activation results in increased pores density of NLAC as the activation leads to evaporation of unstable

ingredients (C present in the form of CO, CO_2, etc.) and activates the binding active sites, respectively [42, 43]. After MB adsorption, the pore cavities were filled up by the dye molecules as a result of which the NLAC surface became smooth and compact. The EDX data after MB adsorption further confirmed that along with C, O and N, elements, S was also present on the NLAC surface. This confirmed that MB dye was removed from the aqueous solution and adsorbs on the NLAC surface.

BET surface area

Figure 6 shows the N_2 adsorption–desorption isotherm and pore size distribution of NL and NLAC, whereas the obtained BET parameters are presented in Table 1. From the table, the NLAC has a high surface of 50.69 m^2/g than the NL of 33.21 m^2/g; this suggested that chemical activation of K_2CO_3 on the NL surface increased the pores density significantly as a result of which surface area increased drastically. The pore size and pore volume of NLAC were 3.5 nm and 0.014 cm^3/g, respectively. The expected average size of MB dye is 0.7×1.7 nm; hence, the MB dye easily accommodates the pores of the NLAC surface and was effectively adsorbed.
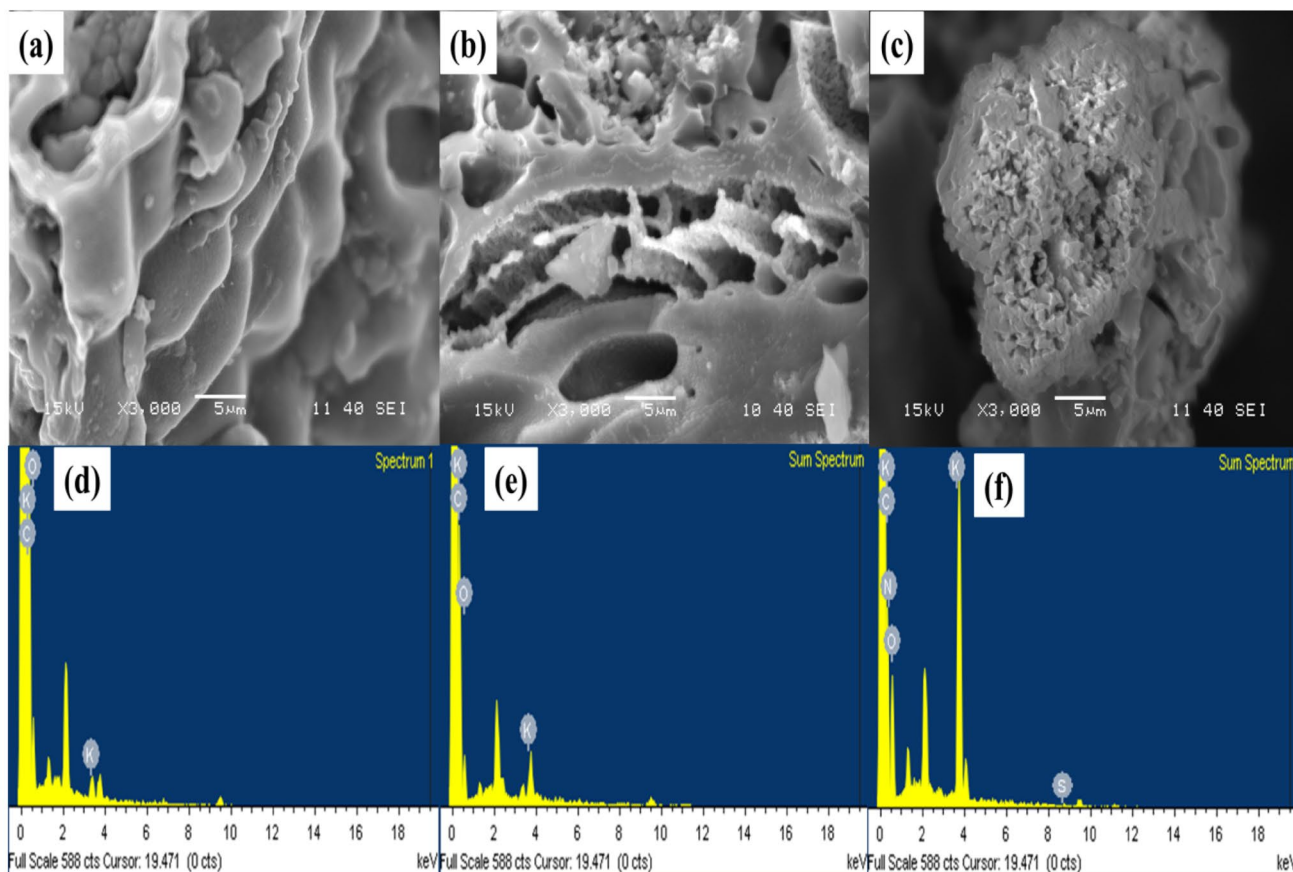

Fig. 5 SEM with corresponding EDX image of NL (**a**, **d**), NLAC (**b**, **e**) and MB dye-adsorbed NLAC (**c**, **f**)
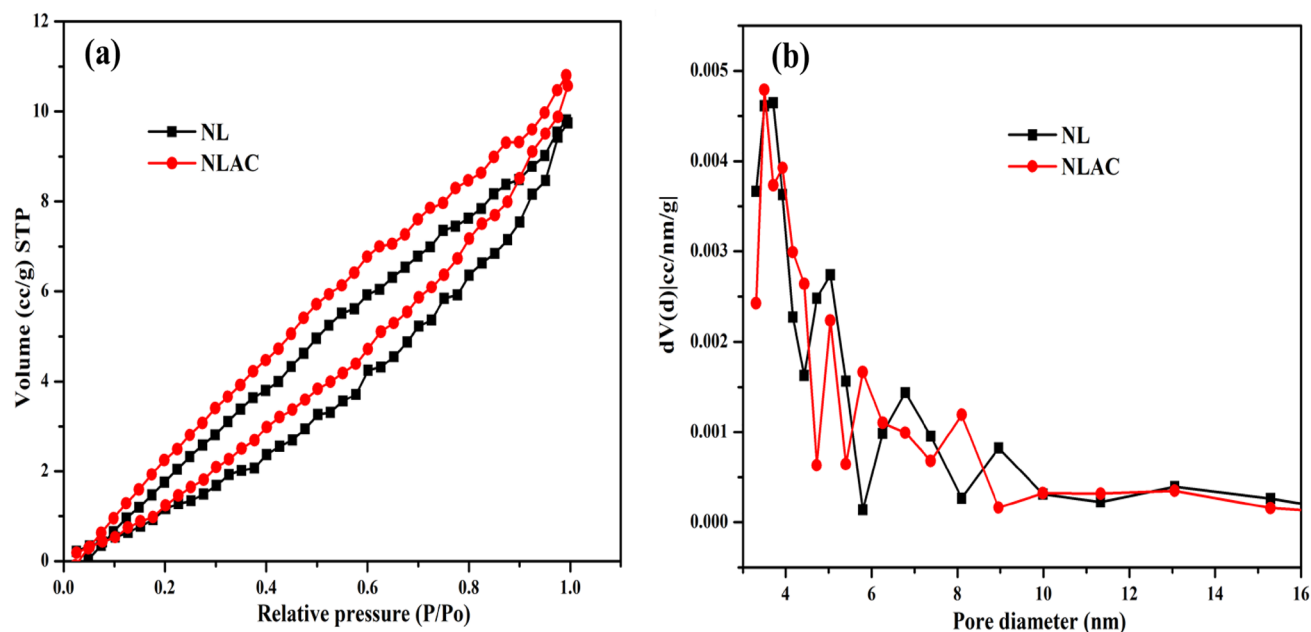
Fig. 6 BET isotherms plot (**a**) and pore size distribution (**b**) of NL and NLAC

Table 1 Details of BET parameters of NL and NLAC

Sample	BET surface area (m^2/g)	Average pore size (nm)	Pore volume (cm^3/g)
NL	33.21	3.7	0.015
NLAC	50.69	3.5	0.014

Removal analysis of MB dye using NLAC

Effect of adsorbent dose

The examination of adsorption dosage is required as it is directly associated with the large-scale application and also for economic study. The effect of NLAC dose was conducted under the conditions of dye concentration 10 mg/L, initial pH 7 and contact time 180 min. The result from the analysis is shown in Fig. 7a. With an alteration in the adsorbent dose from 10 to 100 mg, the MB removal was increased from 30 to 97%. In way of explanation, when the adsorbent dose increases in the solution, the active sites are exposed to dye molecules which require less energy to absorb and thus are absorbed quickly [26]. After the dose of 70 mg, there was no significant change in adsorption efficiency which cleared that after the adsorption dose of 70 mg, all the cationic MB dyes molecules adsorbed onto the surface of the NLAC and the formation of the equilibrium state takes place between the absorbent and the pollutants in the solution.

Effect of dye concentration and contact time

The effect of initial MB dye concentration was studied in the range of 10 to 100 mg/L under room temperature with an adsorbent dose of 70 mg, pH 7 and contact time of 180 min. The outcomes are presented in Fig. 7b, which directed that a decrease in adsorption rate enhanced the initial concentration. This was because the surface area of the adsorbent at a low initial concentration (10 mg/L) and high concentrations (100 mg/L) was the same; hence, the active sites of the adsorbent become completely and immediately saturated, and the remaining dye within the solution was not adsorbed. Therefore, increasing the initial concentration of MB decreased the adsorption capability from 96 to 34%. Further, the effect of contact time was studied in the range of 10–180 min with an initial concentration of 10 mg/L and an adsorbent dose of 70 mg. The outcomes (Fig. 7c) confirmed that at the first contact time, the adsorption of dyes proceeds rapidly, but after 100 min the adsorption rate was nearly constant and not changes necessarily with improved time. This high rate of adsorption in lower time is due to the sufficient surface area and unsaturated active sites for adsorption dye molecules; at the same time, the reaction time was lengthened, and the active sites were occupied, leading to nearly constant adsorption efficiency [25].

Effect of pH

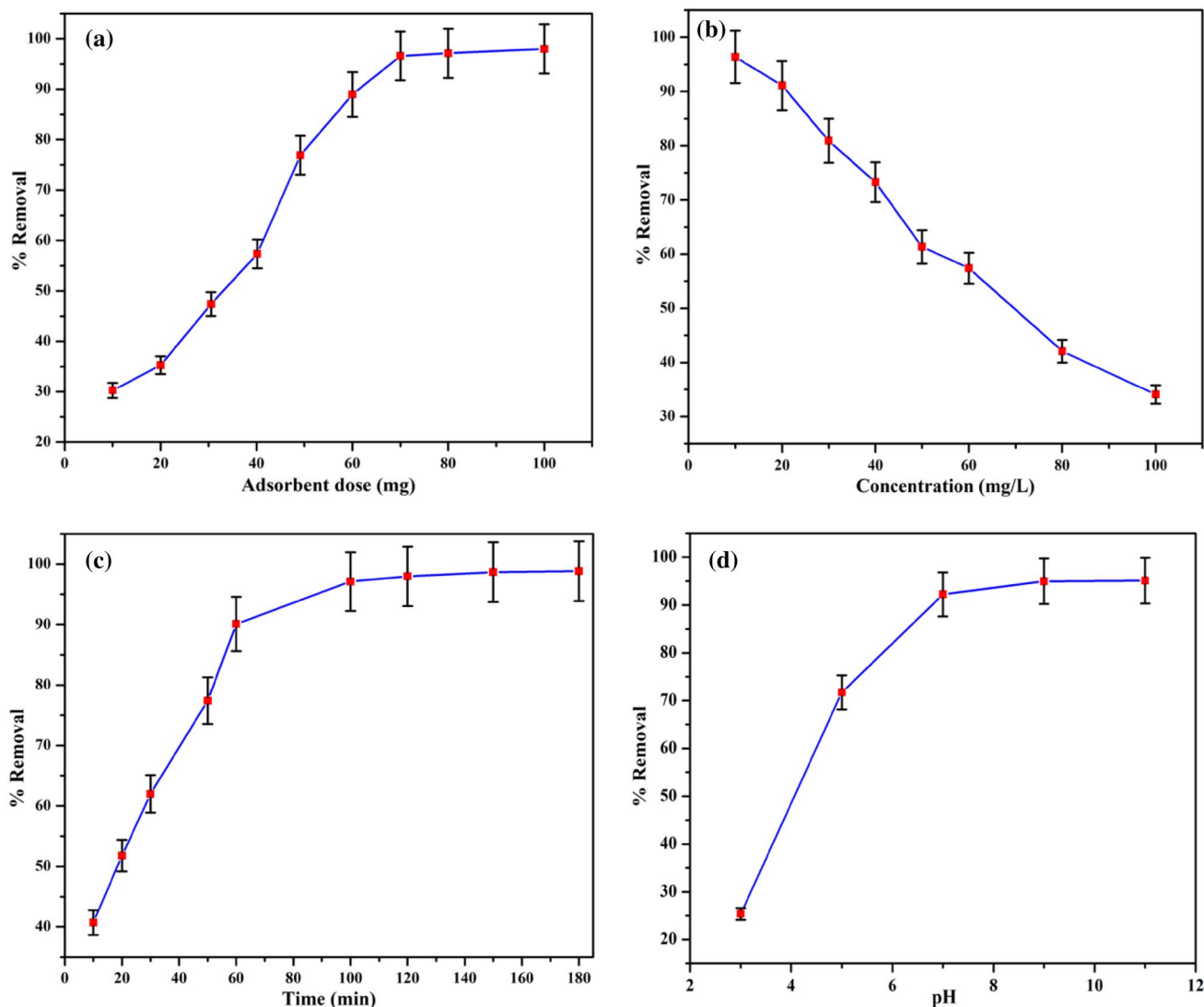pH is an important process parameter in the adsorption work as it influences the surface properties in the

Fig. 7 Influence of adsorbent dose (**a**), initial concentration (**b**), contact time (**c**) and pH (**d**), on the removal of MB dye

adsorption process. The effect of pH on the MB adsorption had been done in the range of 2–11 under the conditions of contact time 100 min, 10 mg/L initial concentration and 70 mg of adsorbent dose, respectively. Results (Fig. 7d) indicated that at lower pH, the oxygen-containing functional group of NLAC surface protonated; as a result, a repulsive electrostatic force occurred with cationic MB dye molecules which decreased the adsorption efficiency. The pHpzc of the material was 6.9, so above this pH adsorbent surface was negatively charged; hence, the removal rate was maximized at higher pH.

Adsorption isotherm

The adsorption isotherm gives information about the adsorption behavior and possible adsorption mechanism and evaluates the adsorption capacity of the adsorbent, respectively.

Three well-known isotherm models were used to express the adsorption behavior of MB dye, i.e., Langmuir [44], Freundlich [45] and Temkin isotherm [46]. The nonlinear equations of the above isotherms model are as follows:

$$q_e = \frac{q_m b C_e}{1 + b C_e} \tag{3}$$

$$q_e = K_F C_e^{1/n} \tag{4}$$

$$q_e = \frac{RT}{Bt} \ln K_T C e \tag{5}$$

Here, R and T are universal gas constant (8.314 J/Kmol) and temperature, q_e is the uptake capacity of adsorbent (mg/g); b, K_F and n are Langmuir constant, Freundlich constant and heterogeneity factor; Bt and K_T are binding energy

constant (J/mol) and Temkin isotherm constant (L/g). Figure 8 presents the nonlinear fitting of the isotherms model with the MB dye adsorption data, and the established isotherms parameters are presented in Table 2. Analysis indicated that the Langmuir isotherms model has higher R^2 values of 0.96 than the Freundlich ($R^2 = 0.85$) and Temkin isotherm ($R^2 = 0.94$) models. The R_L value was also found between 0 and 1, i.e., 0.01 which further supports the data to follow Langmuir isotherm model, respectively. Hence, MB dye molecules were homogeneously distributed on the NLAC surface through the monolayer adsorption process [41]. The adsorption capacity of the present activated carbon was compared with other activated carbon prepared with bio-waste and presented in Table 3. It was observed that the activated carbon prepared from agricultural product has the potential for MB dye removal. The present material has high adsorption capacity and can be applied for wastewater treatments for dyes removal.

Adsorption kinetics

Adsorption kinetics examines the rate between adsorbent and adsorbate and the factors affecting the rate of reaction. In this work, the pseudo-first-order reaction (PFO) and pseudo-second-order reaction (PSO) are used to know the
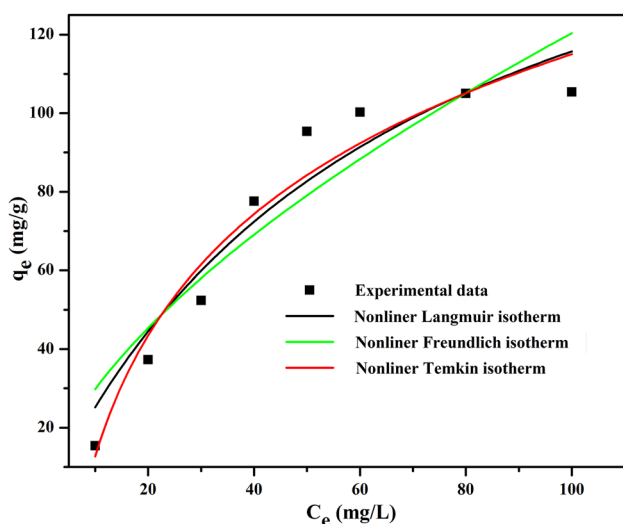

Fig. 8 Nonlinear fitting Langmuir, Freundlich and Temkin adsorption isotherm model

Table 3 Adsorption capacity of different adsorbent materials

Adsorbents	q_m (mg/g)	References
Oil palm frond and palm kernel shell	331.6	[29]
Walnut shell	307.4	[47]
Coconut shell	160.3	[30]
Neem leaves	132.52	Present study
Chickpea stem	96.15	[48]
Coriandrum sativum	94.9	[49]
Bamboo waste	85.6	[50]
Orange and lemon peels	38	[51]
Tamarind Seeds	1.42	[52]

information about the adsorption kinetics of MB dye on the NLAC surface. The nonlinear PFO and PSO kinetics equations are expressed as follows:

$$q_t = q_e\left(1 - e^{-k_1 t}\right) \tag{6}$$

$$q_t = \frac{q_e^2 k_2 t}{1 + q_e k_2 t} \tag{7}$$

where both q_e and q_t are the uptake capacity of adsorbent at equilibrium time and any time t; k_1 and k_2 are rate constants of the first order and second order, respectively. Figure 9 shows the adsorption kinetics plots, and the obtained parameters are presented in Table 4. The determination coefficient (R^2) of the pseudo-second-order kinetics model was 0.96 and higher than the pseudo-first-order kinetic model ($R^2 = 0.95$). Hence, the pseudo-second-order was more suitable than the pseudo-first-order. Thus, it is chemically controlled, which may be showed in the exchange of electrons between NLAC hydrophilic sites and dye cations, respectively [51].

Thermodynamics studies

To calculate the thermodynamic parameters ($\Delta G°$, $\Delta H°$ and $\Delta S°$), batch analysis was carried out in different temperature ranges from 30 to 90 °C at 10 mg/L MB dye concentration, pH 7, contact time 100 min and adsorbent dose 70 mg. Figure 10a indicates that at a rise temperature of 30 to 90 °C the MB dye removal increased from 90.9 to 96.09%, respectively. This indicated that decolonization of dye molecules
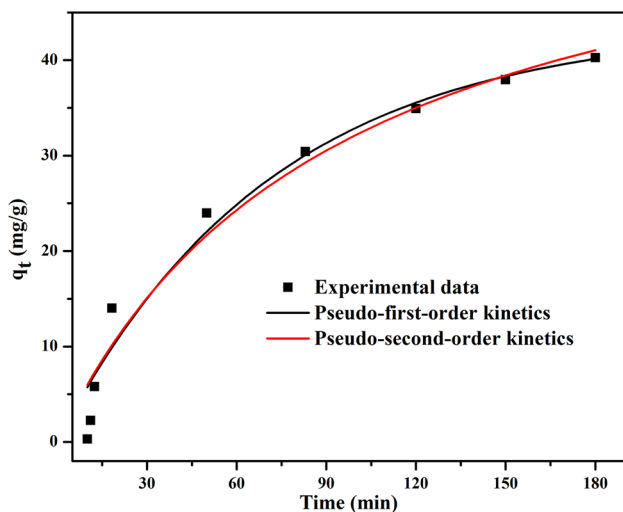
Table 2 Langmuir, Freundlich and Temkin isotherm parameters for MB dye adsorption

		Langmuir isotherm		Freundlich isotherm		Temkin isotherm	
MB dye	q_m(mg/g)	132.52	K_f (mg/g)	7.37	Bt (J/mol)	44.45	
	b(L/mg)	0.12	N	1.64	K_T(L/mg)	0.13	
	R_L	0.01					
	R^2	0.96	R^2	0.85	R^2	0.94	

Fig. 9 Nonlinear fitting of PFO and PSO kinetics model

Table 4 Kinetic parameters and correlation coefficients (R^2) for pseudo-first-order and pseudo-second-order kinetic models

Pseudo-first-order			Pseudo-second-order		
q_t (mg/g)	K_1	R^2	q_t (mg/g)	K_2	R^2
43.59	0.014	0.956	62.58	0.001	0.967

on the NLAC surface was increased with temperature which ultimately increased the rate of adsorption capacity. The optimum temperature was 80 °C as removal of dye became constant after this temperature. Thermodynamics parameters have been analyzed using the following equations:

$$\Delta G = -RT \ln K_C \tag{12}$$

$$\log K_C = \left[\frac{\Delta S}{2.303R} - \frac{\Delta H}{2.303RT} \right], \tag{13}$$

where $\Delta G°$, $\Delta S°$ and $\Delta H°$ symbolize free energy, entropy and enthalpy change and K_C is the thermodynamic distribution coefficient. These parameters were calculated from van't Hoff's linear plot (Fig. 10b), and the results are represented in Table 5. Here, it can be concluded that the MB dye adsorption of NLAC surface was endothermic in nature as further supported by positive values of $\Delta S°$ (0.095 kJ/Kmol) and $\Delta H°$ (0.095 kJ/mol). On the other side, the negative values of $\Delta G°$ indicated the spontaneity of MB dye adsorption on the homogenous surface of NLAC and disorderness on the surface increases with temperature [53].
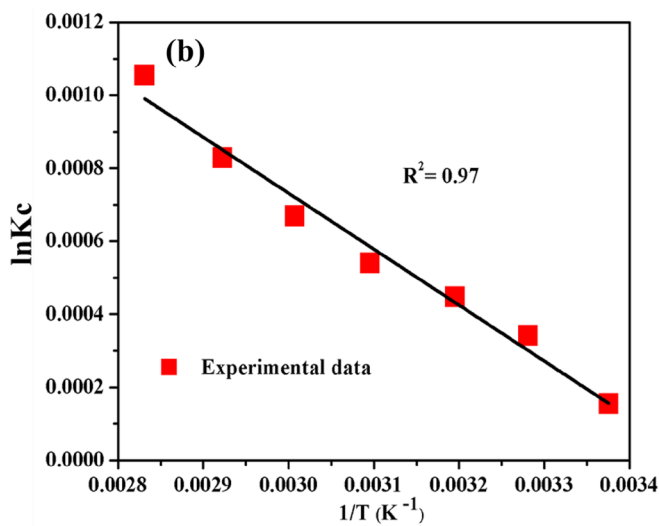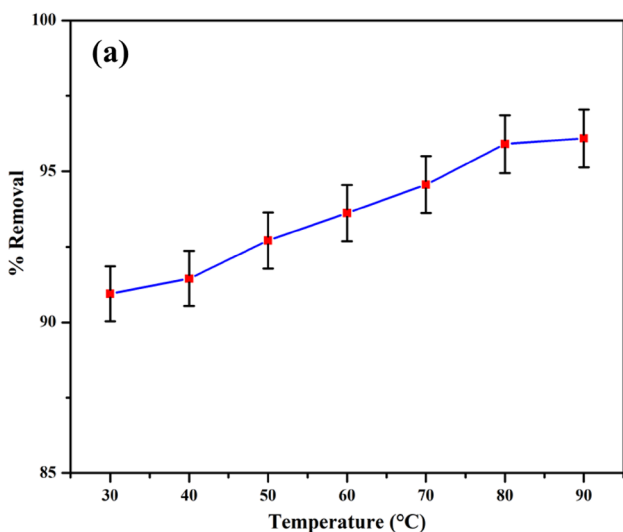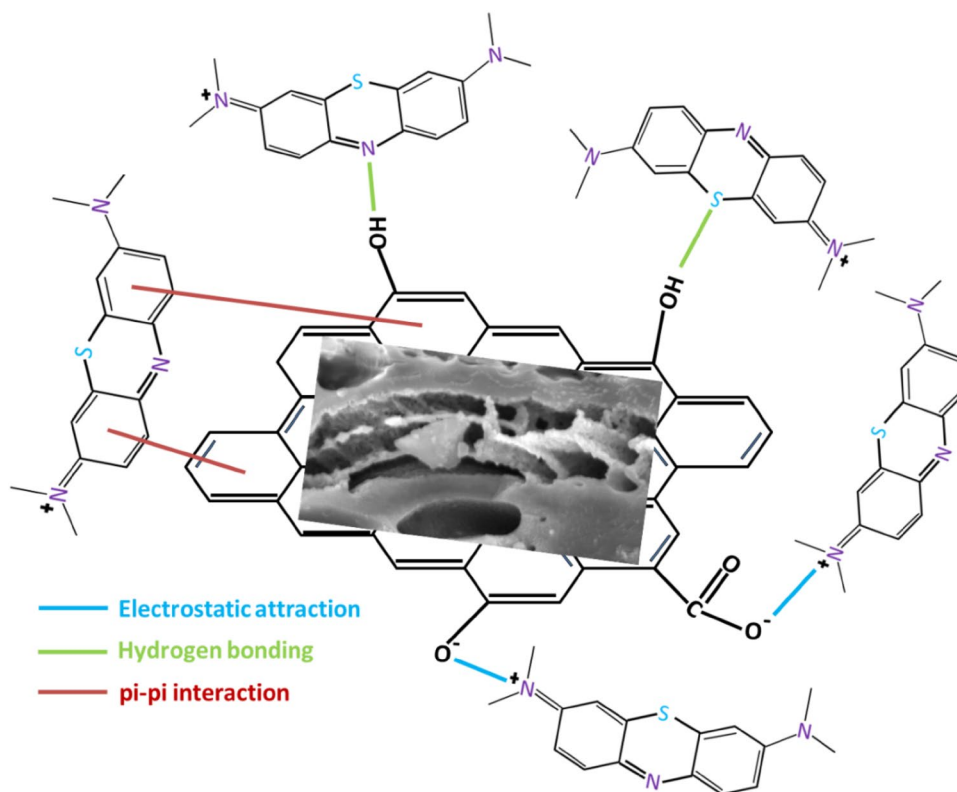

Fig. 10 Effect of temperature **a** van't Hoff plot, **b** for MB removal

Table 5 Obtained thermodynamic parameters for MB dye adsorption

			ΔG (kJ/mol)						
	ΔH (kJ/mol)	ΔS (kJ/Kmol)	303 K	313 K	323 K	333 K	343 K	353 K	363 K
MB	0.029	0.095	−28.75	−29.70	−30.65	−31.60	−32.55	−33.50	−34.45

Fig. 11 Representation of possible interactions mechanism of MB dye on the NLAC surface

Adsorption mechanism

The adsorption of MB dye molecules on the NLAC surface was explained in the results obtained from the FTIR and pH$_{IEP}$ studies. As we have discussed earlier in FTIR studies, shifting in –OH bends took place after adsorption; hence, this suggested that –OH groups of phenol, acid, alcohol and ether were responsible for MB adsorption. Based on these, three types of adsorption mechanisms were proposed as presented in Fig. 11. Firstly, it was found that the pH$_{IEP}$ of NLAC was 6.9, so above this pH adsorbent surface is negatively charged and attracts the positively charged dye molecules. Secondly, hydrogen bonding was carried out between the –OH and –COOH groups of adsorbent with the N and S atoms of the MB dye molecules. Lastly, electron donor–acceptor pi–pi interaction was seen between the aromatic rings of MB dyes and the pi-electron system of activated carbon, respectively.

Conclusion

Here, the activated carbon was prepared using a biomass waste of neem leaf which not only reduces environmental pollution but is also reused for the application of wastewater treatment. The K$_2$CO$_3$ activation by microwave process bought significant results in activated carbon formation from NL powder. The formed NLAC had a surface area of 50.69 m^2/g. In the optimized conditions of 10 mg/L initial MB dye concentration, pH 8, contact time 100 min, temperature 80 °C and adsorbent dose of 70 mg, about 97% of MB dye was removed from the aqueous solution. The MB dye adsorption on the NLAC surface was proceeding with the Langmuir isotherm model with an uptake capacity of 132.52 mg/g. The removal data matched with the pseudo-second-order kinetic model which indicated the chemisorption process. Hence, the NLAC can be applied to a real-life application for MB dye removal in wastewater treatment.

References

1. M. Irani, M.M. Ghafurian, M.M. Khorasani, R. Mehrkhah, O. Mahian, J. Taiwan Inst. Chem. Eng. **128**, 253 (2021)
2. K.E. Ukhurebor, K.R. Singh, V. Nayak, G. UK-Eghonghon, Environ. Sci. Process. Impacts. **23**, 1060 (2021)
3. K.E. Ukhurebor, P.A. Aidonojie, Agric. Food Secur. **10**, 1 (2021)
4. W. Nwankwo, K.E. Ukhurebor, I.O.P. Conf, Ser. Earth Environ. Sci. **655**, 012018 (2021)

5. G.O. Ogunlusi, O.D. Amos, O.F. Olatunji, A.A. Adenuga, J. Iran. Chem. Soc. **20**, 817 (2023)
6. F. Yang, J. Zhang, T. Lin, L. Ke, L. Huang, S.P. Deng, J. Zhang, S. Tan, Y. Xiong, M. Lu, J. Iran. Chem. Soc. **20**, 801 (2023)
7. F. Benali, B. Boukoussa, I. Ismail, M. Hachemaoui, J. Iqbal, I. Taha, Z. Cherifi, A. Mokhtar, Surf. Interfaces **26**, 101306 (2021)
8. M. Thakur, G. Sharma, T. Ahamad, A.A. Ghfar, D. Pathania, M. Naushad, Coll. Surf. B Biointerfaces **157**, 456 (2017)
9. T. A. Yousef, U. K. Sahu, A. H. Jawad, N. N. Abd Malek, O. K. Al Duaij, and Z. A. ALOthman, Int. J. Phytoremediation (2022)
10. B. Lellis, C.Z. Fávaro-Polonio, J.A. Pamphile, J.C. Polonio, Biotechnol. Res. Innov. **3**, 275 (2019)
11. T.M. Eldeeb, U.O. Aigbe, K.E. Ukhurebor, R.B. Onyancha, M.A. El-Nemr, M.A. Hassaan, S. Ragab, O.A. Osibote, A. El Nemr, Biomass Convers. Biorefinery (2022)
12. S. Ihaddaden, D. Aberkane, A. Boukerroui, D. Robert, J. Water Process Eng. **49**, 102952 (2022)
13. Y. Guesmi, H. Agougui, R. Lafi, M. Jabli, A. Hafiane, J. Mol. Liq. **249**, 912 (2018)
14. S.A. Kordkandi, M. Forouzesh, J. Taiwan Inst. Chem. Eng. **45**, 2597 (2014)
15. F.J. Tuli, A. Hossain, A.K.M.F. Kibria, A.R.M. Tareq, S.M.M.A. Mamun, A.K.M.A. Ullah, Environ. Nanotechnol. Monit. Manag. **14**, 100354 (2020)
16. K. Goharshadi, S.A. Sajjadi, E.K. Goharshadi, R. Mehrkhah, Mater. Res. Bull. **154**, 111916 (2022)
17. M. Aziznezhad, E.K. Goharshadi, R. Mehrkhah, M.M. Ghafurian, Mater. Res. Bull. **149**, 111705 (2022)
18. M. Karimi-Nazarabad, E.K. Goharshadi, Sol. Energy Mater. Sol. Cells **160**, 484 (2017)
19. M. Karimi-Nazarabad, E.K. Goharshadi, S.J. Mahdizadeh, J. Phys. Chem. C **123**, 26106 (2019)
20. S. Alkaykh, A. Mbarek, E.E. Ali-Shattle, Heliyon **6**, e03663 (2020)
21. H.M. Mashhoor, M. Eftekhari, N. Rezazadeh, M.K. Nazarabad, Nanotechnol. Environ. Eng. **8**, 75 (2023)
22. A.H. Jawad, U.K. Sahu, M.S. Mastuli, Z.A. ALOthman, L.D. Wilson, Biomass Convers. Biorefinery (2022)
23. Z. Aksu, Process Biochem. **40**, 997 (2005)
24. S.A. Gupta, Y. Vishesh, N. Sarvshrestha, A.S. Bhardwaj, P.A. Kumar, N.S. Topare, S. Raut-Jadhav, S.A. Bokil, A. Khan, Mater. Today Proc. **57**, 1500 (2022)
25. H. Xue, X. Wang, Q. Xu, F. Dhaouadi, L. Sellaoui, M.K. Seliem, A. Ben Lamine, H. Belmabrouk, A. Bajahzar, A. Bonilla-Petriciolet, Z. Li, Q. Li, Chem. Eng. J. **430**, 132801 (2022)
26. S. Sahu, S. Pahi, S. Tripathy, S.K. Singh, A. Behera, U.K. Sahu, R.K. Patel, J. Mol. Liq. **315**, 113743 (2020)
27. M. Chandrakala, Int. J. Res. Appl. Sci. Eng. Technol. **6**, 480 (2018)
28. S. Giraldo, N.Y. Acelas, R. Ocampo-Pérez, E. Padilla-Ortega, E. Flórez, C.A. Franco, F.B. Cortés, A. Forgionny, Molecules **27**, 5105 (2022)
29. K. Jasri, A.S. Abdulhameed, A.H. Jawad, Z.A. Alothman, T.A. Yousef, O.K. Al Duaij, Diam. Relat. Mater. **131**, 109581 (2023)
30. I. Kurnia, S. Karnjanakom, I. Irkham, H. Haryono, Y.A. Situmorang, A. Indarto, A.R. Noviyanti, Y.W. Hartati, G. Guan, RSC Adv. **13**, 220 (2022)
31. A. Yaqub, S.M. Syed, H. Ajab, M. Zia Ul Haq, J. Environ. Manag. **327**, 116925 (2023)
32. N.T. Abdel-Ghani, G.A. El-Chaghaby, M.H. Elgammal, E.S.A. Rawash, New Carbon Mater. **31**, 492 (2016)
33. H. Deng, G. Li, H. Yang, J. Tang, J. Tang, Chem. Eng. J. **163**, 373 (2010)
34. H. Sayğılı, G.A. Sayğılı, J. Clean. Prod. **226**, 968 (2019)
35. I.P. Da Paixão Cansado, C. Ramiro Belo, P.A. Mira Mourão, Environ. Nanotechnol. Monit. Manag. **12**, 100261 (2019)
36. L. Wang, F. Sun, F. Hao, Z. Qu, J. Gao, M. Liu, K. Wang, G. Zhao, Y. Qin, Chem. Eng. J. **383**, 123205 (2020)
37. G. Pandhare, N. Trivedi, N. Kanse, S.D. Dawande, Int. J. Adv. Eng. Res. Stud. **2**, 29 (2013)
38. S. Kumari, S.H.K. Annamareddy, Environ. Dev. Sustain. **22**, 2967 (2020)
39. M. Prabhu, S. Ruby Priscilla, K. Kavitha, P. Manivasakan, V. Rajendran, P. Kulandaivelu, Biomed. Res. Int. **2014**, 1 (2014)
40. A. Suhaimi, A.S. Abdulhameed, A.H. Jawad, T.A. Yousef, O.K. Al Duaij, Z.A. Alothman, L.D. Wilson, Diam. Relat. Mater. **130**, 109456 (2022)
41. K.Y. Foo, B.H. Hameed, Bioresour. Technol. **104**, 679 (2012)
42. M. Auta, B.H. Hameed, Chem. Eng. J. **175**, 233 (2011)
43. M.A. Ahmad, N. Ahmad, O.S. Bello, Appl. Water Sci. **5**, 407 (2015)
44. I. Langmuir, J. Am. Chem. Socity **38**, 2221 (1916)
45. H. Freundlich, J. Phys. Chem. **57**, 384 (1906)
46. M.I. Temkin, V. Pyzhev, Acta Physiochim. URSS **12**, 327 (1940)
47. A. Vakili, A.A. Zinatizadeh, Z. Rahimi, S. Zinadini, P. Mohammadi, S. Azizi, A. Karami, M. Abdulgader, J. Clean. Prod. **382**, 134899 (2023)
48. N. Genli, S. Kutluay, O. Baytar, Ö. Şahin, Int. J. Phytoremediation **24**, 88 (2022)
49. C.C. de Souza, L.Z.M. de Souza, M. Yılmaz, M.A. de Oliveira, A.C. da Silva Bezerra, E.F. da Silva, M.R. Dumont, A.R.T. Machado, Clean. Mater. **3**, 100052 (2022)
50. A. Fyrdaus Khaizuran Zahari, U.K. Sahu, T. Khadiran, S.N. Surip, Z.A. Alothman, A.H. Jawad, Separations **9**, 390 (2022)
51. D. Ramutshatsha-Makhwedzha, A. Mavhungu, M.L. Moropeng, R. Mbaya, Heliyon **8** (2022)
52. Z. Ishak, S. Salim, D. Kumar, Trop. Aquat. Soil Pollut. **2**, 1 (2022)
53. S. Sahu, S. Pahi, J.K. Sahu, U.K. Sahu, R.K. Patel, Environ. Sci. Pollut. Res. **27**, 22579 (2020)